Electronic Supplementary Material (ESI) for Soft Matter

Supplementary Information for "Nanomechanics measurements of live bacteria reveal a mechanism for bacterial cell protection: the polysaccharide capsule in *Klebsiella* is a responsive polymer hydrogel that adapts to osmotic stress"

Huabin Wang, Jonathan J. Wilksch, Trevor Lithgow, Richard A. Strugnell, and Michelle L. Gee*

* To whom correspondence should be addressed. E-mail: mlgee@unimelb.edu.au

Cell viability test

Cell viability was assessed using a LIVE/DEAD BacLight Viability Kit (Molecular Probes). Wild type and capsule mutant *K. pneumoniae* cells were adhered to modified glass discs (same as the sample preparation for the AFM experiments) and submerged in either Milli-Q or 100 mM $CaCl_2$ solutions for three time points and then treated with SYTO 9 and propidium acid nucleic acid stains. SYTO 9 stains live and dead cells fluorescent green, whereas propidium acid stains dead cells fluorescent red. Thus, with an appropriate mixture of the SYTO9 and propidium iodide stains, bacteria with intact cell membranes stain fluorescent green, whereas bacteria with damaged membranes stain fluorescent red. Cells were visualised with an inverted fluorescence microscope (Leica, DM14000B) and imaged with a Leica DFC350FX digital camera. Images were processed with Adobe Photoshop CS5.1 for Mac. In our tests, we found that the ratio of damaged cells (red) to viable, intact cells (green) is below 5%. This means that the cells, both wild type and capsule-deficient mutants, remain viable, with no change in viability, under all solution conditions used in the study for at least the duration of an experiment. Typical images for three time points are shown in **Figs. S1-S3**.

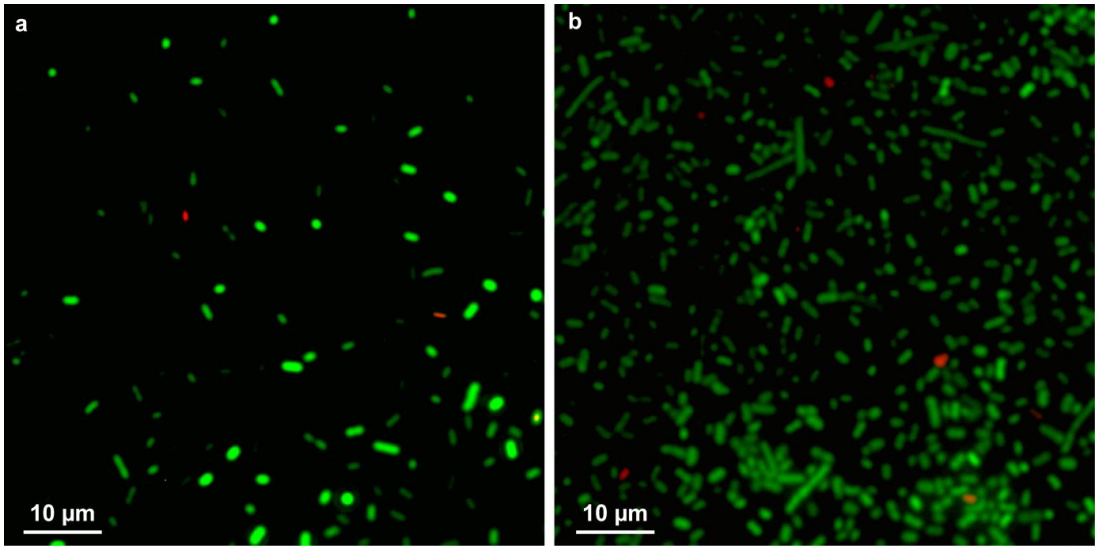

Fig. S1 Fluorescence images of wild- type (a) and capsule-deficient (b) *Klebsiella pneumoniae* taken immediately after the samples were treated with a LIVE/DEAD BacLight Viability Kit.

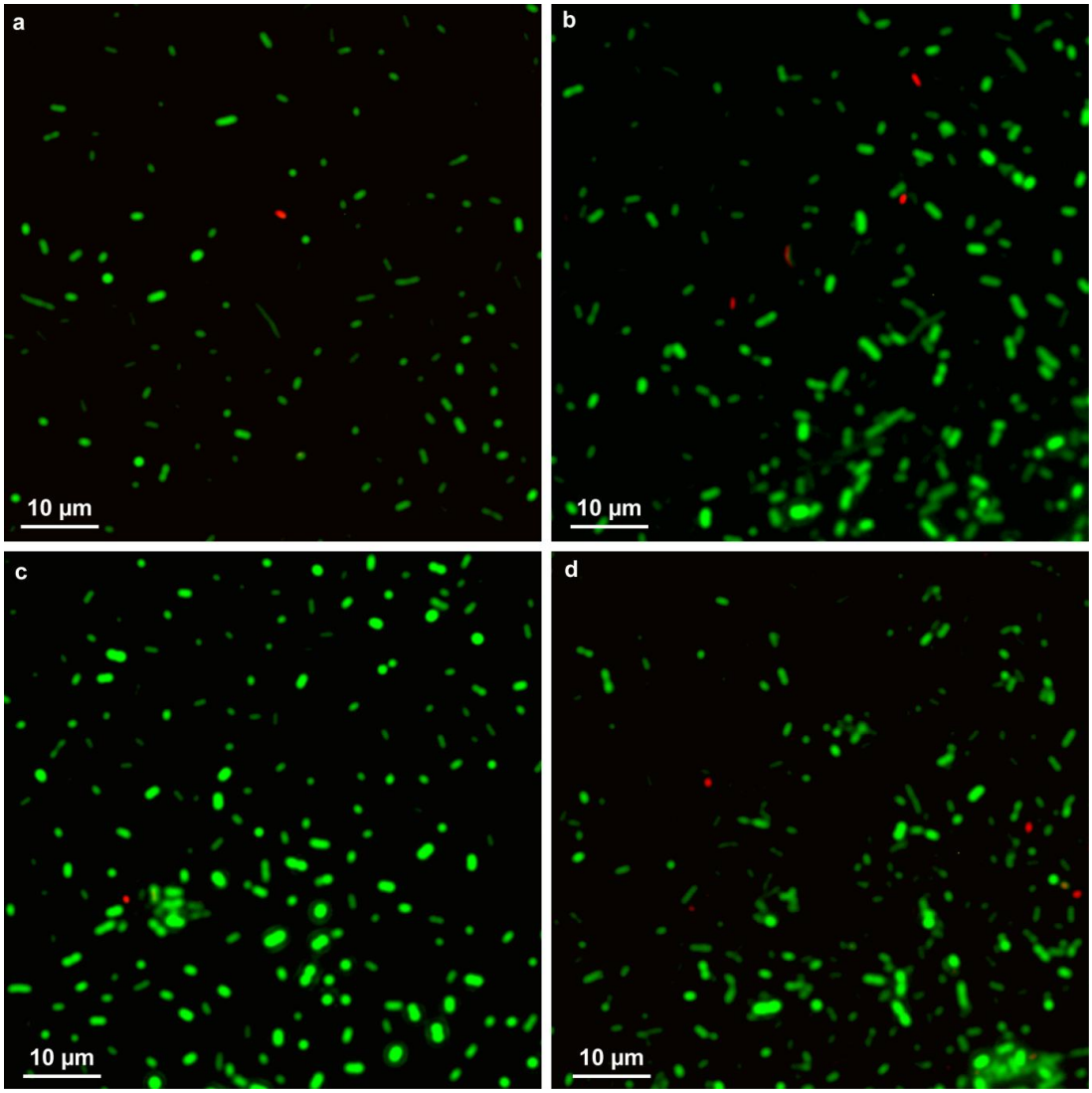

Fig. S2 Fluorescence images taken after 4 hours immersion of wild type and capsule-deficient mutants of *Klebsiella pneumoniae* in either Milli-Q water or $CaCl_2$ (100 mM) and subsequently treated with a LIVE/DEAD BacLight Viability Kit. (a) wild type bacteria in Milli-Q water; (b) capsule-deficient bacteria in Milli-Q water; (c) wild type bacteria in $CaCl_2$ solution; (d) capsule-deficient bacteria in $CaCl_2$ solution.

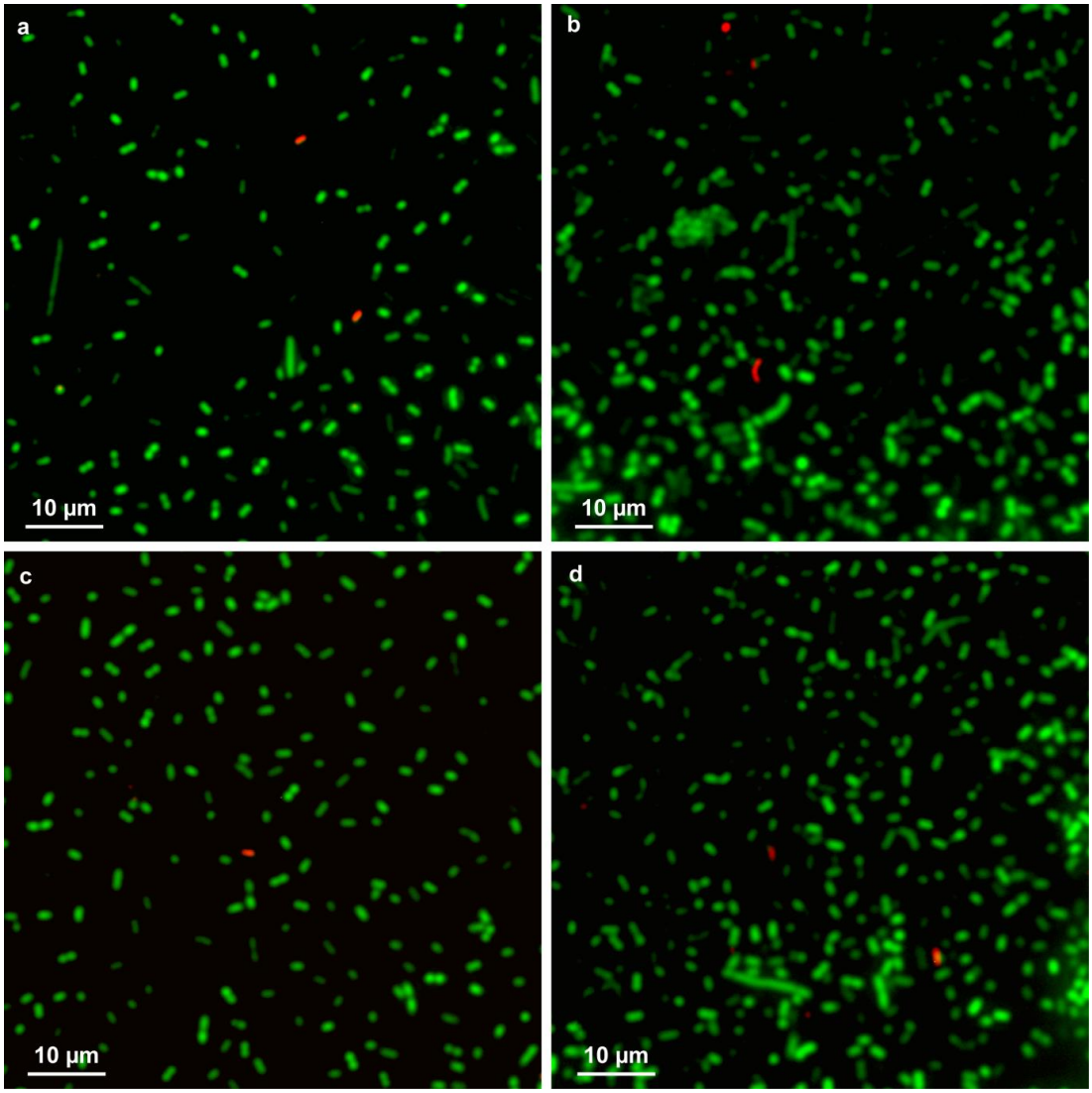

Fig. S3 Fluorescence images taken after 7 hours immersion of wild type and capsule-deficient mutants of *Klebsiella pneumoniae* in either Milli-Q water or $CaCl_2$ (100 mM) and subsequently treated with a LIVE/DEAD BacLight Viability Kit. (a) wild type bacteria in Milli-Q water; (b) capsule-deficient bacteria in Milli-Q water; (c) wild type bacteria in $CaCl_2$ solution; (d) capsule-deficient bacteria in $CaCl_2$ solution.

Cell dimensions

Cell dimensions were determined from AFM images for each cell type. The numbers quoted are averages over all cells in a scan for 5-7 different samples per cell type.

Cell type	Height (nm)	Length (nm)	Width (nm)
Wild- type in Milli-Q water	703± 61	2660± 353	2158± 290
Wild- type in $CaCl_2$ solution	712±75	2283±303	1574±167
Capsule-deficient in Milli-Q water	892±70	2671±267	1787±150
Capsule-deficient in $CaCl_2$ solution	719±190	2360±295	1751±73

Force curve reproducibility

In our expreiments, force curves collected on individual bacteria are highly reproducible. We illustrate this in **Fig. S4,** which show 10 force curves for particular samples overlayed in single plots. As stated in the manuscript, for a specific sample, 150-210 force profiles at different points along the apex of cells were collected to provide statistics. The overlay of all 150-210 force profiles for each frame of **Fig. S4** would appear as a single thick line so we limit our plots to 10 force profiles each, to best highlight data reproducibility.

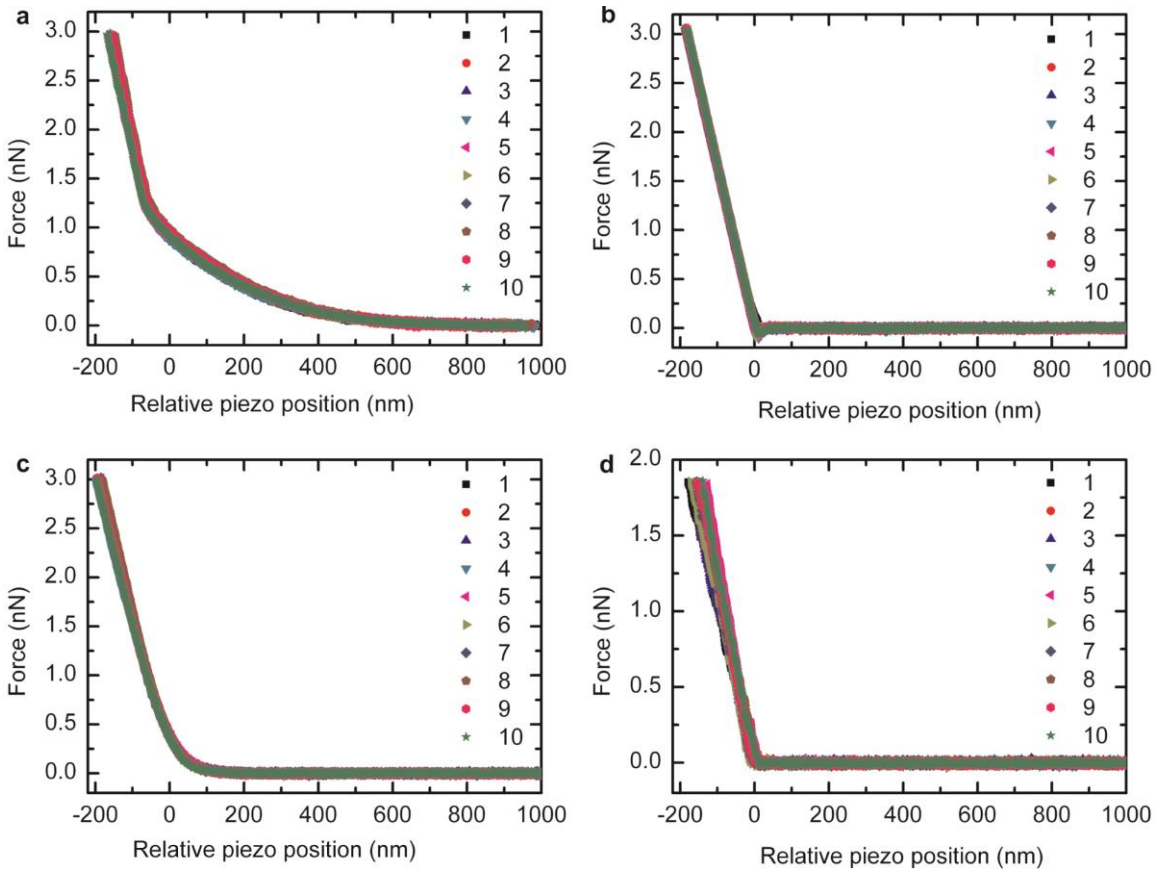

Fig. S4 Representative force profiles for the interaction of the AFM tip at the apical surface of individual wild type and capsule deficient *K. pneumoniae* AJ218 bacteria in Milli-Q™ water: (a) is the wild type and (b) is capsule-deficient, and in 100 mM calcium chloride solution: (c) is the wild type and (d) is capsule-deficient. Each plot contains 10 different measured force profiles that overlay each other, highlighting the high reproducibility of the measurements.

AFM images of the bacterial cell surface

Small scan size AFM images were taken of each cell type (wild type and capsule-deficient) under all solution conditions used in the study. The images were all similar in that the surfaces of the cells appear smooth (approximately 5 nm rms roughness) and featureless. Note that fimbriae are not detected. LPS and fimbriae constitute the surface polymers in the capsule-deficient mutatants. These also are not detected. This is likely due to the fluidity of the surface polymers *in situ*.

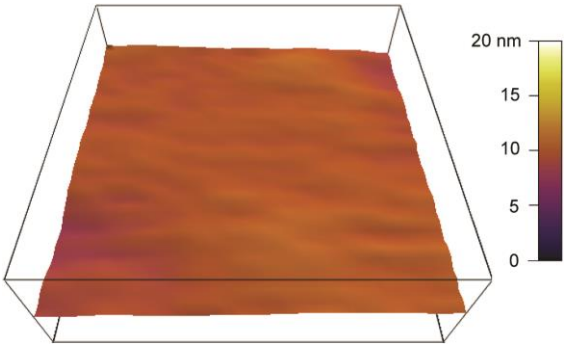

Fig S5. AFM contact-mode 3D height image of live, wild-type *K. pneumonia AJ218* cells in Milli-Q^{TM} water. The cells are adhered to polyethyleneimine-coated glass disks. The legend to the right shows the relative height, in nm, of features in the image. Scan size: 200 nm × 200 nm.

Structure of Capsule polysaccharide in *Klebsiella pneumoniae* serotype K54

The serotype we study is K54. It has been shown (*G.S. Dutton and E.H. Merrifield, Carbohydrate Research 1982, 105, 189-203*) that the primary structure is:

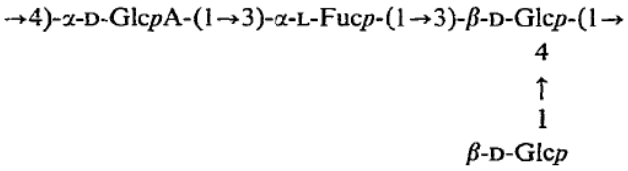

with an octasaccharide repeat unit:

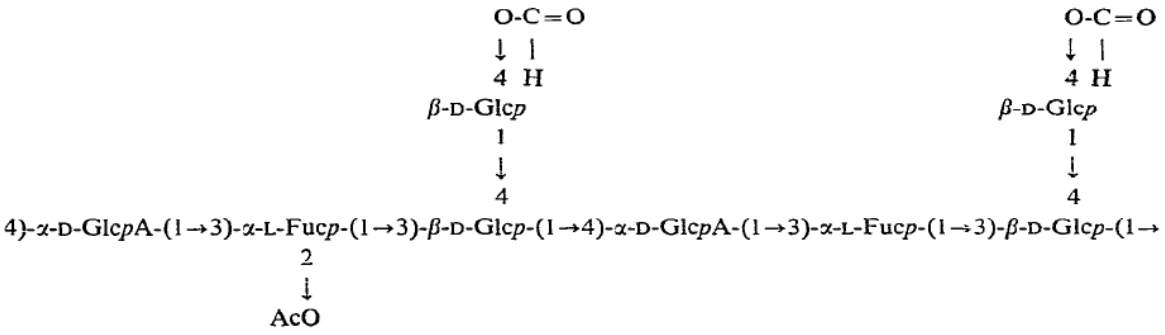

The Hertz Equation

We followed the method used by Manfred Radmacher[4] and Michelle Oyen. [5] When a conical indenter presses into an elastic half-space, the force can be expressed by

$$F_{loading} = \frac{\pi}{2} \times \frac{E}{\left(1-\upsilon^2\right)} \times r^2 \times \tan(\theta) \qquad \text{(A)}$$

Where E is Young's modulus, υ is the Poisson ratio, r is the contact radius and θ is the angle formed by the indenter and the plane of the compressed surface.[6]

The indentation depth δ can be related to contact radius r by two methods: that of Manfred Radmacher[4] and Michelle Oyen[5] who use $\delta = r \times \tan(\theta)$[4, 5]; or that of Weisenhorn *et al.*[7] and Wu *et al.*[6] who use $\delta = \pi/2 \times r \times \tan(\theta)$. Both ways are acceptable.

We followed the method used by Radmacher[4] and Oyen[5], so we can obtain equation (3) in the manuscript, viz:

$$F_{loading} = \frac{\pi}{2} \times \frac{E}{\left(1-\upsilon^2\right)} \times \delta^2 \times \tan(\alpha) \qquad \text{(B)}$$

where α is the half- opening angle of the cone, and $\alpha = \pi/2 - \theta$.

If following the method used by Weisenhorn et al.[7] and Wu et al.[6] one can obtain the expression:

$$F_{loading} = \frac{2}{\pi} \times \frac{E}{\left(1-\upsilon^2\right)} \times \frac{\delta^2}{\tan(\theta)} \qquad \text{(C)}$$

which can be rearranged to:

$$F_{loading} = \frac{2}{\pi} \times \frac{E}{\left(1-\upsilon^2\right)} \times \delta^2 \times \tan(\alpha) \qquad \text{(D)}$$

For these two methods, the coefficients in the equations are different: $\pi/2$ is obtained in the derivation of equation (B), and $2/\pi$ is obtained in the derivation of equation (D). Note that the selection of either (B) or (D) in fitting force profile data does not influence the form of the fitted equation but yields different Young's moduli, since the terms in π are only constant coefficients to their respective forms of the Hertz equation.

Data fitting

The experimental data were fitted to user-defined functions (Eqs 1 – 4 in the manuscript) using the iterative procedure of Levenberg-Marquardt algorithm, coded in-house in Igor Pro (Version 6.04, Wavemetrics Inc., USA). The estimates of initial values for unknown variables were restricted in the first instance to physically meaningful values. The parameters that yielded the lines of best fit to the data were selected as those for which chi-squared was minimised.

The uncertainty of a model fit to data is commonly evaluated by using prediction bands at 95% confidence interval.[1, 2] The prediction bands were calculated via:[3]

$$\hat{Y} \pm t_{(v,1-\alpha/2)}\sqrt{\sigma^2 + V(\hat{Y})}$$

where $\hat{Y}$ is the predicted value of the model at a given value of the independent variable X, $V(\hat{Y})$ is the variance of a predicted model value, and σ^2 is the sample variance. The function $t_{(v,\ 1-\alpha/2)}$ is the value on a Student's t-distribution with v degrees of freedom.

At the 95% confidence level, 95% of the experimentally measured data points should fall within the prediction bands. In each of our fittings, more than 95% of the data points fall within the prediction bands and are reasonably well distributed within the prediction bands (e.g. **Figs. S6 and S7**). Each of the fitted lines well superimposes on the corresponding experimental data under the Cartesian coordinate system as described in the manuscript.

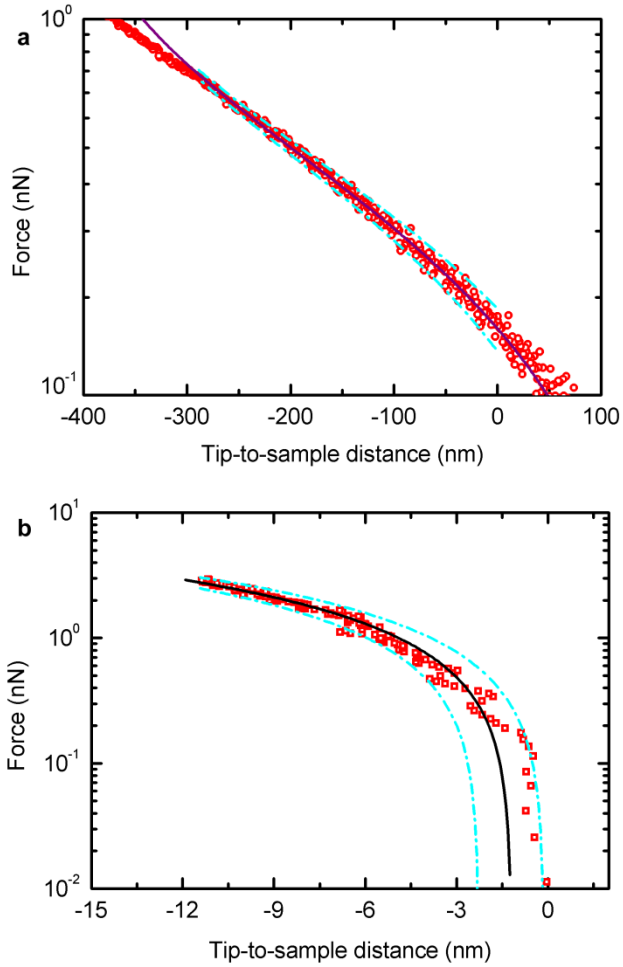

Fig. S6 Prediction bands with 95% confidence intervals (cyan dashed lines) for (a) Pincus fit (purple line) for wild type, and (b) the Hooke's law fit (black line) for capsule-deficient bacteria in Milli-Q™ water.

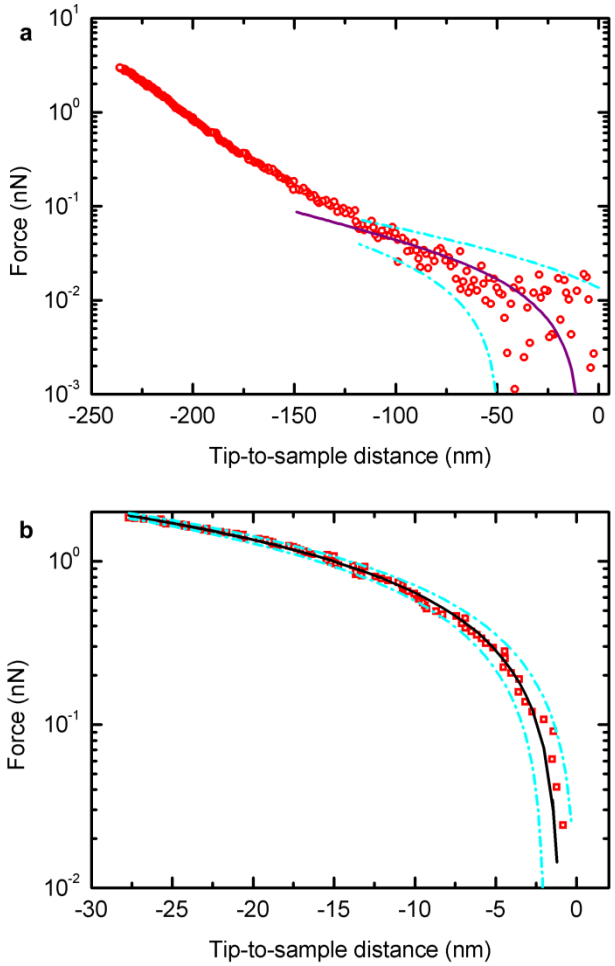

Fig. S7 Prediction bands with 95% confidence intervals (cyan dashed lines) for (a) Pincus fit (purple line) for wild type, and (b) the Hooke's law fit (black line) for capsule-deficient bacteria in 100 mM $CaCl_2$ aqueous solution.

1. G. G. S. Dutton and E. H. Merrifield, *Carbohyd. Res*., 1982, **105**, 189-203..
2. M. Radmacher, *Ieee Eng Med Biol*, 1997, **16**, 47-57.
3. M. L. Oyen, *Exp Techniques*, 2013, **37**, 73-87.
4. H. W. Wu, T. Kuhn and V. T. Moy, *Scanning*, 1998, **20**, 389-397.
5. A. L. Weisenhorn, M. Khorsandi, S. Kasas, V. Gotzos and H. J. Butt, *Nanotechnology*, 1993, **4**, 106-113.
6. D. C. G. Klein, K. M. Ovrebo, E. Latz, T. Espevik and B. T. Stokke, *J Mol Recognit*, 2012, **25**, 74-81.
7. H. J. Motulsky and A. Christopoulos, GraphPad Software Inc., San Diego CA, www.graphpad.com., Second edn., 2003, p. 32.
8. J. O. Rawlings, S. G. Pantula and D. A. Dickey, *Applied Regression Analysis: A Research Tool*, Springer-Verlag New York, Inc., 1998.